Measurements of the Decay $K_L \to e^+e^-\gamma$

E. Abouzaid,[4] M. Arenton,[10] A. R. Barker,[5,*] L. Bellantoni,[7] E. Blucher,[4] G. J. Bock,[7] E. Cheu,[1] R. Coleman,[7] M. D. Corcoran,[9] B. Cox,[10] A. R. Erwin,[11] A. Glazov,[4] A. Golossanov,[10] Y. B. Hsiung,[7] D. A. Jensen,[7] R. Kessler,[4] H. G. E. Kobrak,[3] K. Kotera,[8] J. LaDue,[5] A. Ledovskoy,[10] P. L. McBride,[7] E. Monnier,[4,†] H. Nguyen,[7] R. Niclasen,[5] E. J. Ramberg,[7] R. E. Ray,[7] M. Ronquest,[10] J. Shields,[10] W. Slater,[2] D. Smith,[10] N. Solomey,[4] E. C. Swallow,[4,6] P. A. Toale,[5] R. Tschirhart,[7] Y. W. Wah,[4] J. Wang,[1] H. B. White,[7] J. Whitmore,[7] M. J. Wilking,[5,‡] R. Winston,[4] E. T. Worcester,[4] T. Yamanaka,[8] and E. D. Zimmerman[5]

[1]*University of Arizona, Tucson, Arizona 85721, USA*
[2]*University of California at Los Angeles, Los Angeles, California 90095, USA*
[3]*University of California at San Diego, La Jolla, California 92093, USA*
[4]*The Enrico Fermi Institute, The University of Chicago, Chicago, Illinois 60637, USA*
[5]*University of Colorado, Boulder, Colorado 80309, USA*
[6]*Elmhurst College, Elmhurst, Illinois 60126, USA*
[7]*Fermi National Accelerator Laboratory, Batavia, Illinois 60510, USA*
[8]*Osaka University, Toyonaka, Osaka 560-0043 Japan*
[9]*Rice University, Houston, Texas 77005, USA*
[10]*The Department of Physics and Institute of Nuclear and Particle Physics, University of Virginia, Charlottesville, Virginia 22901, USA*
[11]*University of Wisconsin, Madison, Wisconsin 53706, USA*

(Received 23 February 2007; published 3 August 2007)

The E799-II (KTeV) experiment at Fermilab has collected 83 262 $K_L \to e^+e^-\gamma(\gamma)$ events above a background of 79 events. We measure a decay width, normalized to the $K_L \to \pi^0\pi^0\pi^0_D$ ($\pi^0 \to \gamma\gamma$, $\pi^0 \to \gamma\gamma$, $\pi^0_D \to e^+e^-\gamma(\gamma)$) decay width, of $\Gamma(K_L \to e^+e^-\gamma(\gamma))/\Gamma(K_L \to \pi^0\pi^0\pi^0_D) = (1.3302 \pm 0.0046_{\text{stat}} \pm 0.0102_{\text{syst}}) \times 10^{-3}$. We also measure parameters of two $K_L\gamma^*\gamma$ form factor models. In the Bergström-Massó-Singer parametrization, we find $C\alpha_{K^*} = -0.517 \pm 0.030_{\text{stat}} \pm 0.022_{\text{syst}}$. We separately fit for the first parameter of the D'Ambrosio-Isidori-Portolés model and find $\alpha_{\text{DIP}} = -1.729 \pm 0.043_{\text{stat}} \pm 0.028_{\text{syst}}$.

DOI: 10.1103/PhysRevLett.99.051804 PACS numbers: 13.20.Eb, 14.40.Aq

The rare decay $K_L \to e^+e^-\gamma$ offers a direct means for studying the dynamics of the $K_L\gamma^*\gamma$ vertex. The form factor of this vertex is important for determining the long-distance, two photon contribution to the $K_L \to \mu^+\mu^-$ decay width so that the more interesting short-distance contributions can be determined. These contributions have been important for extracting a direct constraint on the real part of the CKM matrix parameter V_{td} [1,2]. In addition, this short-distance information provides one of the most stringent constraints on flavor-changing neutral-current couplings of the Z boson, which are beyond the standard model [1]. In this Letter we present a measurement of the $K_L\gamma^*\gamma$ form factor and $K_L \to e^+e^-\gamma$ branching ratio using data from the 1997 run of the E799-II (KTeV) experiment at Fermilab.

Two parametrizations of the form factor are considered. The first model, proposed by Bergström, Massó, and Singer (BMS), describes the $K_L\gamma^*\gamma$ vertex in terms of two types of processes: a K_L transition into a π^0, η, η' state that decays to two photons, and a vector meson dominance contribution in which the K_L first decays into a K^* and a photon followed by a strangeness changing vector-vector transition into a ρ, ω, ϕ state that decays into a virtual photon [3]. The relative size of these two contributions is characterized by a constant parameter, $C\alpha_{K^*}$. The BMS form factor model, given in Eq. (1), is a function of the Dalitz variable x, which is defined as the squared ratio of the e^+e^- mass to the K_L mass.

$$f_{\text{BMS}}(x) = \frac{1}{1 - x\frac{M_K^2}{M_\rho^2}} + \frac{C\alpha_{K^*}}{1 - x\frac{M_K^2}{M_{K^*}^2}}\left(\frac{4}{3} - \frac{1}{1 - x\frac{M_K^2}{M_\rho^2}} - \frac{1}{9} \times \frac{1}{1 - x\frac{M_K^2}{M_\omega^2}} - \frac{2}{9}\frac{1}{1 - x\frac{M_K^2}{M_\phi^2}}\right). \quad (1)$$

The form factor model proposed by D'Ambrosio, Isidori, and Portolés (DIP) is a slightly more general model that applies to all $K_L\gamma^*\gamma^*$ vertices [4].

$$f_{\text{DIP}}(x_1, x_2) = 1 + \alpha_{\text{DIP}}\left(\frac{x_1}{x_1 - \frac{M_\rho^2}{M_K^2}} + \frac{x_2}{x_2 - \frac{M_\rho^2}{M_K^2}}\right) + \beta_{\text{DIP}}\frac{x_1 x_2}{(x_1 - \frac{M_\rho^2}{M_K^2})(x_2 - \frac{M_\rho^2}{M_K^2})}. \quad (2)$$

The variables x_1 and x_2 are the squared ratios of the masses of the two virtual photons to the kaon mass. The $K_L \to e^+e^-\gamma$ decay is only sensitive to α_{DIP} since one of the photons emerging from the vertex is real.

The E799 phase of the KTeV experiment focused 800 GeV protons from the Tevatron at Fermilab onto a BeO target. The resulting particles were collimated into two parallel neutral beams. The beams passed through a 65 m vacuum decay region beginning 94 m downstream of the target. Immediately following the decay region was a charged track spectrometer. It consisted of two upstream drift chambers, a dipole magnet, and two downstream drift chambers. The drift chambers achieved a position resolution of about 100 μm, which corresponded to a momentum resolution of $\sigma(P)/P = 0.38\% \oplus 0.016\% \times P(\mathrm{GeV}/c)$. Both the decay pipe and charged spectrometer were surrounded by lead-scintillator photon veto detectors.

A transition radiation detector (TRD) consisted of eight planes of polypropylene felt, each followed by a multiwire proportional chamber (MWPC) containing an 80%–20% mixture of Xe and CO_2. The TRD provided a single track pion rejection of better than 200:1 at 90% electron efficiency [5].

A CsI electromagnetic calorimeter was just downstream of the TRD. The calorimeter provided an energy resolution of $\sigma(E)/E = 0.45\% \oplus 2\%/\sqrt{E(\mathrm{GeV})}$. Behind the calorimeter was a muon system consisting of planes of lead, steel, and scintillator. More detailed descriptions of the KTeV detector can be found elsewhere [6,7].

A $K_L \to e^+e^-\gamma$ event was observed in the KTeV detector as two oppositely charged tracks in the charged spectrometer that each pointed to a cluster in the calorimeter, and a third calorimeter cluster corresponding to the photon. Each cluster was required to have an energy greater than 2.75 GeV, and for electrons the ratio, E/p, of cluster energy (measured by the calorimeter) to track momentum (measured by the spectrometer) was required to lie between 0.925 and 1.075 to discriminate against muon and pion backgrounds. Several cuts were made to ensure that the decay vertex was inside the fiducial region and to remove events near the edge of a detector. A vertex χ^2 cut required that the decay particles originated from a common vertex, and a χ^2 cut on track matching at the center of the analysis magnet ensured that the tracks were well-reconstructed. The total kaon energy was required to be between 40 and 200 GeV, and less than 0.15 GeV of energy was allowed in each of the photon veto counters.

Since all of the final state particles in this decay mode were reconstructed, it was possible to impose two additional kinematic constraints. The first was a cut on the square of the component of the reconstructed kaon momentum transverse to the original kaon direction (p_t^2). A cut on p_t^2 was placed at 500 $(\mathrm{MeV}/c)^2$ to reduce events with extra particles not related to the decay and events with missing decay particles. The other kinematic constraint was the requirement that the reconstructed kaon mass lie between 0.475 GeV/c^2 and 0.520 GeV^2.

One of the main backgrounds was from $K_L \to \pi^\pm e^\mp \nu_e$ (K_{e3}) decays with either an accidental or radiated photon. In order for these events to mimic a signal, the pion had to be misidentified as an electron. This occurred when most of its energy was deposited in the calorimeter yielding an E/p value close to 1. The K_{e3} background peaked below the signal in reconstructed $e^+e^-\gamma$ mass, which is consistent with the kinematic limit of 0.477 GeV/c^2 for an event with a pion misidentified as an electron. This background was significantly reduced by requiring a TRD pion probability of less than 5% for each track. Figure 1 shows a plot of the $e^+e^-\gamma$ invariant mass before and after the TRD cut.

The other main background was due to $K_L \to \gamma\gamma$ events where one of the photons converted into an e^+e^- pair while exiting the vacuum region. Since these photon conversions yielded e^+e^- tracks that tended to be close together upon reaching the charged spectrometer, requiring a separation of 1.5 mm in the x or y view of the first drift chamber of the charged spectrometer effectively removed these events. In a Monte Carlo simulation of 10 times the expected number of $K_L \to \gamma\gamma$ conversion events, no events survived this cut.

To measure the branching ratio, the $K_L \to e^+e^-\gamma$ rate was normalized to the rate of $K_L \to \pi^0\pi^0\pi^0_D$ ($K_L \to \pi^0\pi^0\pi^0$ with two subsequent $\pi^0 \to \gamma\gamma$ decays and one $\pi^0 \to e^+e^-\gamma$ decay). To reconstruct this mode, two tracks pointing to clusters in the calorimeter and five additional photon clusters were required. To determine which four photons belonged to the two $\pi^0 \to \gamma\gamma$ decays, the decay vertex position was calculated for each pair of photons using the separation distance and energies of the corresponding clusters, and assuming that they came from a π^0. A pairing χ^2 was then constructed based on the requirement that both π^0 particles had the same vertex position. The photon pairing that yielded the smallest χ^2 was assumed to be correct. The remaining photon was assumed to come from the $\pi^0 \to e^+e^-\gamma$ decay. Photon mispairing occurred a small fraction of the time, but this effect was well reproduced in the Monte Carlo simulation.

The cuts used to isolate $K_L \to \pi^0\pi^0\pi^0_D$ events were kept as similar as possible to those used for $K_L \to e^+e^-\gamma$ with a

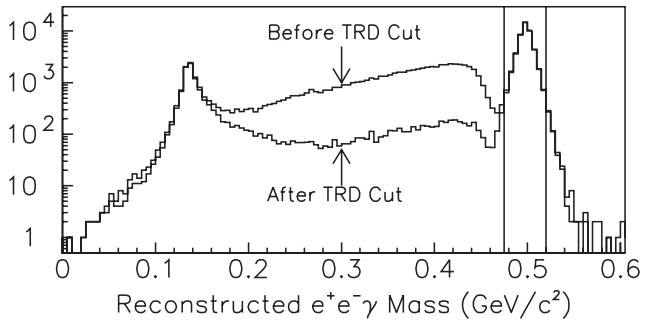

FIG. 1. The reconstructed $e^+e^-\gamma$ mass distribution before and after the TRD cut shows a significant decrease in the amount of background while retaining most of the signal. The signal region is indicated by the two vertical lines centered on the kaon mass.

few exceptions. The four additional photons in the final state significantly improved the total kaon mass resolution, so the kaon mass cuts were tightened to 0.485 GeV/c^2 and 0.510 GeV/c^2. A loose cut was made on the photon pairing χ^2, and after matching the remaining photon with the e^+e^- pair, a cut was made on the $e^+e^-\gamma$ mass to select the region between 0.1275 GeV/c^2 and 0.1425 GeV/c^2.

The only significant background to the decay $K_L \to \pi^0\pi^0\pi^0_D$ was from $K_L \to \pi^0\pi^0\pi^0$ events where one of the photons converted to an e^+e^- pair. This background was removed with the same track separation requirement used in the signal mode.

Monte Carlo simulations were used to determine the acceptances of the signal and normalization decay modes. Both modes used the same event generator as the KTeV $K_L \to e^+e^-\gamma\gamma$ measurement [8], which included $\mathcal{O}(\alpha^2)$ radiative corrections in the calculation of the decay width [9]. Without radiative corrections the measured branching ratio would have been shifted by 1.7%.

To implement $\mathcal{O}(\alpha^2)$ corrections, a cutoff of $m_{\gamma\gamma} = 1$ MeV/c^2 was introduced to distinguish $K_L \to e^+e^-\gamma$ from the radiative decay, $K_L \to e^+e^-\gamma\gamma$. For events below the cutoff, the second photon was not generated. The value of the cutoff was chosen so that the energy of the softer photon in $K_L \to e^+e^-\gamma\gamma$ events near the cutoff would be too low to be detected. The detector acceptance for $K_L \to e^+e^-\gamma(\gamma)$ events was found to be 3.4%. For $K_L \to \pi^0\pi^0\pi^0_D$ events, the acceptance was 0.26%.

For the purposes of the branching ratio measurement, the decay $K_L \to e^+e^-\gamma$ can be defined as either all $K_L \to e^+e^-\gamma$ and $K_L \to e^+e^-\gamma\gamma$ events (the inclusive definition), or by introducing a cutoff to distinguish $K_L \to e^+e^-\gamma$ from $K_L \to e^+e^-\gamma\gamma$ (the exclusive definition). We report our results using both of these definitions. For the exclusive result, $K_L \to e^+e^-\gamma$ is defined as all events where the softer photon has an energy less than 5 MeV in the kaon rest frame ($E^{\rm cm}_{\gamma 2} < 5$ MeV). This definition is chosen to coincide with previous measurements of the $K_L \to e^+e^-\gamma\gamma$ branching ratio [8].

The same definitional ambiguity also exists for the normalization mode. Since previous measurements of $\pi^0 \to e^+e^-\gamma$ have been inclusive [10], using the inclusive definition as the normalization mode allows one to extract more easily the absolute value of the $K_L \to e^+e^-\gamma$ branching ratio.

Since the normalization mode had four more photons than the signal mode, the largest systematic uncertainty was the absolute photon inefficiency in the calorimeter. The three sources of photon detection bias considered were the calorimeter geometry simulation, the simulated photon energy spectrum, and the electromagnetic shower containment. To measure the effect of the simulated calorimeter geometry, the outer edge of the calorimeter was moved by 0.5 mm in the $K_L \to \pi^0\pi^0\pi^0_D$ Monte Carlo events only. This resulted in a 0.226% variation in the branching ratio. The photon energy simulation was tested by shifting the Monte Carlo photon energies by 10 MeV, which caused the branching ratio to vary by 0.219%. These variations were chosen based on detector survey data and information from other decay modes. Finally, an upper bound on the effect of imperfect electromagnetic shower containment in the calorimeter was found by studying the low-end tail of the E/p distribution for electrons. Both $K_L \to \pi^\pm e^\mp \nu_e$ events and $K_L \to \pi^0\pi^0\pi^0$ events were used to find best-fit shapes for the low-end E/p tail. Switching between these two shapes in the Monte Carlo simulation caused a variation of 0.288% in the branching ratio. These three effects, added in quadrature, resulted in a 0.43% systematic uncertainty.

The inefficiency of the drift chambers was also a source of systematic uncertainty. Two-dimensional inefficiency maps of each drift chamber were measured using $K_L \to \pi^\pm e^\mp \nu_e$ decays. These inefficiency maps were then adjusted by a constant factor to give the best agreement between the data and the Monte Carlo simulation. One sigma variations about the best-fit value for this factor yielded a 0.37% systematic error on the branching ratio.

An overall systematic uncertainty due to disagreements between the data and the Monte Carlo simulation was measured by studying the effect of varying the analysis cuts. The cut values on many important quantites were studied, such as the vertex position, E/p, energy in the photon vetos, reconstructed mass, pion probability, minimum photon energy, and total energy. These variations resulted in a 0.33% variation in the branching ratio.

There was also a systematic uncertainty due to the simulation of the kaon energy spectrum. The ratio of the total kaon energy distributions between the data and the Monte Carlo simulation exhibited a slope in both the signal and normalization modes. The slope was corrected by reweighting the Monte Carlo events based on total kaon

TABLE I. Uncertainties for the $K_L \to e^+e^-\gamma$ branching ratio and form factor parameter measurements.

Branching ratio uncertainties	% of BR	$\Delta\, C\alpha_{K^*}$	$\Delta\, \alpha_{\rm DIP}$
Statistical uncertainty	0.33%	0.030	0.038
BR ($K_L \to \pi^0\pi^0\pi^0_D$) uncertainty	2.83%	N/A	N/A
Absolute γ inefficiency	0.43%	N/A	N/A
Drift chamber inefficiency	0.37%	0.009	0.011
Cut variations	0.33%	0.013	0.016
Kaon energy spectrum	0.23%	0.011	0.014
Trigger inefficiency	0.21%	N/A	N/A
Calorimeter energy resolution	0.14%	0.001	0.001
Background level	0.08%	0.000	0.000
Detector material	0.07%	0.008	0.009
Drift chamber hit resolution	0.04%	0.002	0.003
$\mathcal{O}$ (α^3) Radiative corrections	0.03%	0.008	0.009
Form factor dependence	0.03%	N/A	N/A
Total systematic uncertainty	0.77%	0.022	0.028

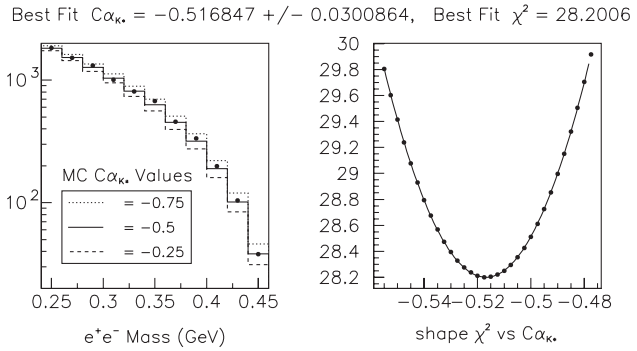

FIG. 2. The variation in the shape of the e^+e^- mass distribution was used to determine the values of the form factor parameters. Three comparisons between data (dots) and Monte Carlo samples (histograms) with different values of $C\alpha_{K^*}$ are shown as well as the final fit to the shape χ^2 values. Of the 23 e^+e^- mass bins used in the fit, only the highest 11 are shown.

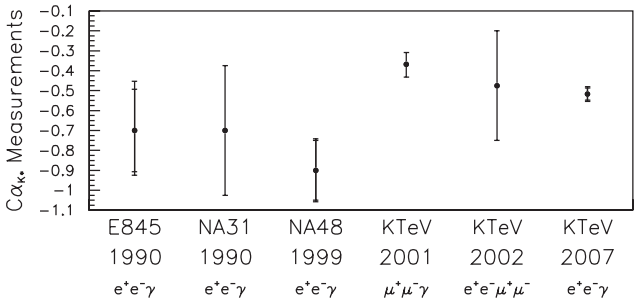

FIG. 3. The graph shows a comparison of our measurement of $C\alpha_{K^*}$ with previous measurements. The outer error bars represent the total uncertainty and the inner error bars are the statistical uncertainty only (where applicable) [12–16].

energy. The reweighted Monte Carlo events were used for the central value measurement, and the variation in the branching ratio due to reweighting, 0.23%, was treated as a systematic uncertainty.

Several other smaller systematic effects have been evaluated as well. The full list of systematic uncertainties is given in Table I.

We have observed 83 262 $K_L \to e^+e^-\gamma(\gamma)$ events over a background of 79 events. Using 4 924 801 $K_L \to \pi^0\pi^0\pi^0_D$ events to normalize the $K_L \to e^+e^-\gamma(\gamma)$ rate, the inclusive ($K_L \to e^+e^-\gamma + K_L \to e^+e^-\gamma\gamma$) and exclusive ($E^{\rm cm}_{\gamma 2} < 5$ MeV) ratios of the two K_L decay widths have been measured to be

$$\frac{\Gamma(e^+e^-\gamma)_{\rm inc}}{\Gamma(\pi^0\pi^0\pi^0_D)_{\rm inc}} = (1.3302 \pm 0.0046 \pm 0.0102) \times 10^{-3},$$

$$\frac{\Gamma(e^+e^-\gamma)_{\rm exc}}{\Gamma(\pi^0\pi^0\pi^0_D)_{\rm inc}} = (1.2521 \pm 0.0044 \pm 0.0097) \times 10^{-3},$$

$$\frac{\Gamma(e^+e^-\gamma)_{\rm exc}}{\Gamma(\pi^0\pi^0\pi^0_D)_{\rm exc}} = (1.2798 \pm 0.0045 \pm 0.0099) \times 10^{-3}.$$

Using the known values of BR($K_L \to \pi^0\pi^0\pi^0$), BR($\pi^0 \to \gamma\gamma$) and BR($\pi^0 \to e^+e^-\gamma)_{\rm inc}$ [11], the absolute $K_L \to e^+e^-\gamma$ branching ratio (BR) is

$$\mathrm{BR}_{\rm inc} = (9.128 \pm 0.032 \pm 0.070 \pm 0.252) \times 10^{-6},$$

$$\mathrm{BR}_{\rm exc} = (8.591 \pm 0.030 \pm 0.066 \pm 0.238) \times 10^{-6}.$$

The third error listed is an external systematic error due to the uncertainty in the $K_L \to \pi^0\pi^0\pi^0_D$ branching ratio. These results are in good agreement with all previous measurements with a factor of 3 improvement in the uncertainty on the ratio [12–14].

Since both form factor models being considered are functions of the Dalitz variable x, the shape of the e^+e^- mass distribution is very sensitive to the form factor parameters. Thus, each form factor parameter was extracted by comparing the shape of the e^+e^- mass spectrum in data to several Monte Carlo samples with differing form factor parameter values. A few such comparisons are shown in Fig. 2. For each comparison, a bin-by-bin shape-χ^2 value was calculated. A quadratic fit to these χ^2 values was used to determine each form factor parameter. This fitting procedure was performed separately for the two form factor parameters since the two models depend on x differently.

The uncertainties associated with the form factor measurement are shown in Table I. Unlike the branching ratio uncertainties, the form factor uncertainties are reported as a variation in the measurement, not as a percentage of the final result, since a measurement of zero has no special significance. The method for determining these uncertainties was the same as for the branching ratio.

The final fit for the form factor parameters $C\alpha_{K^*}$ and $\alpha_{\rm DIP}$ yield

$$C\alpha_{K^*} = -0.517 \pm 0.030 \pm 0.022,$$

$$\alpha_{\rm DIP} = -1.729 \pm 0.043 \pm 0.028.$$

The first uncertainty is from the χ^2 minimization fit and the second is the total systematic uncertainty.

Previous measurements of the BMS form factor have been reported in terms of α_{K^*}, where the constant parameter C has been divided out. Since the expression for C involves several experimental quantities that have not been treated consistently in the past, we report $C\alpha_{K^*}$ to avoid confusion. Using previous measurements of α_{K^*} and their corresponding values of C, a comparison with our measured value of $C\alpha_{K^*}$ is shown in Fig. 3. In recent years, the proper value for $C\alpha_{K^*}$ has been unclear due to a 3.1σ difference between the two previous best measurements. Our measurement lies between these values: 2.0σ below the KTeV $K_L \to \mu^+\mu^-\gamma$ result and 2.4σ above the NA48 $K_L \to e^+e^-\gamma$ result.

*Deceased.

[†]Permanent address: C.P.P. Marseille/C.N.R.S., France.
[‡]To whom correspondence should be addressed.

[1] G. Isidori and R. Unterdorfer, J. High Energy Phys. 01 (2004) 009.
[2] M. Gorbahn and U. Haisch, Phys. Rev. Lett. **97**, 122002 (2006).
[3] L. Bergström, E. Massó, and P. Singer, Phys. Lett. B **131**, 229 (1983).
[4] G. D'Ambrosio, G. Isidori, and J. Portolés, Phys. Lett. B **423**, 385 (1998).
[5] G. Graham, Ph.D. thesis, University of Chicago, 1999.
[6] A. Alavi-Harati *et al.*, Phys. Rev. Lett. **83**, 922 (1999).
[7] A. Alavi-Harati *et al.*, Phys. Rev. D **61**, 072006 (2000).
[8] A. Alavi-Harati *et al.*, Phys. Rev. D **64**, 012003 (2001).
[9] K. O. Mikaelian and J. Smith, Phys. Rev. D **5**, 1763 (1972).
[10] M. A. Schardt *et al.*, Phys. Rev. D **23**, 639 (1981).
[11] W.-M. Yao *et al.*, J. Phys. G **33**, 1 (2006).
[12] K. Ohl *et al.*, Phys. Rev. Lett. **65**, 1407 (1990).
[13] G. D. Barr *et al.*, Phys. Lett. B **240**, 283 (1990).
[14] V. Fanti *et al.*, Phys. Lett. B **458**, 553 (1999).
[15] A. Alavi-Harati *et al.*, Phys. Rev. Lett. **87**, 071801 (2001).
[16] A. Alavi-Harati *et al.*, Phys. Rev. Lett. **90**, 141801 (2003).